ARTICLE

The tris-oxovanadium pyrogallate complex: synthesis, structure, magnetic and electronic properties

Received 00th January 20xx,
Accepted 00th January 20xx

DOI: 10.1039/x0xx00000x

Hassan Mkhadder, [a] Morgane Denis,[a] Mónica Giménez-Marqués,[b] Walter Cañón Mancisidor,[c] Bernard Humbert,[a] Elise Deunf,[a] Philippe Poizot,[a] and Thomas Devic *[a]

With the aim at identifying new cation-phenolate complexes, we here investigated the reactivity of pyrogallol (H_3pgal) with vanadium salts. A trimetallic anionic complex was identified, and found to be formed in a broad set of reaction conditions. This complex, formuled V_3O_3(pgal)$_3$ consists of three oxovanadium(IV) connected together by three pyrogallate ligands to afford a bowl-shaped specie presenting a pseudo 3-fold symmetry axis. Its crystal structure is reported, as well as its characterisation by a broad set of techniques, including powder X-ray diffraction, thermogravimetric analysis, infrared and Raman spectroscopies, and solid state UV-visible diffuse reflectance. Its redox activity both in solution and in the solid state is described, together with its magnetic behavior. Eventually, the relevance of this trimetallic unit in the field of phenolic-based biocoatings and MOFs synthesis is briefly discussed.

Introduction

Phenolics and their derived coordination complexes are of importance in a variety of fields, including bioinorganic chemistry, soil (de)contamination, cultural heritage, and materials science. For the latter, bio-inspired bulk materials and coatings, notably made of naturally occurring phenolic building blocks, are especially appealing because they combine a high chemical tunability with interesting electronic and mechanical properties, as well as a good biocompatibility.[1–3] Our physico-chemical understanding of these complex amorphous systems usually relies on the precise chemical and structural information gained from model crystalline molecular complexes. Whereas such a knowledge is rather well established for 1,2-dioxobenzenes (catecholates, cat^{2-}) as well as their oxidised forms (semiquinonate and benzoquinone),[4] it has been less addressed for the 1,2,3-trioxobenzene (pyrogallate, pgal^{3-}) unit, although this motif is found in numerous bio-related phenolics.[2,5]

Even if polymetallic entities have been described,[6–9] catecholate is known to generally favour the formation of monometallic complexes bearing 2 to 3 chelating ligands. In contrast, for pyrogallate, the few reported crystal structures indicate that such a ligand strongly favours the formation of polymetallic entities, each pyrogallol unit being able to easily bind to 2 cations (see Scheme 1). Whatever the oxidation state and the ionic radius of the cation, small, planar and highly symmetric pyrogallol derivatives were found to mostly drive to the formation of infinite chain-like motifs,[10–19] whereas bulkier ligands presenting a bent geometry seem to favour the formation of molecular entities.[20–25] More precisely, the reactivity of C-alkylpyrogallol[4]arenes or PgC_n, (tetra-pyrogallol derivatives) was deeply investigated, notably by Atwood *et al.* It was found that giant molecular capsules build up from six ligands and triangular trimetallic units could be produced with a broad range of divalent, trivalent and tetravalent cations (Mg(II),[26] V(IV),[27] Mn(III/II),[23] Fe(III/II),[24] Co(II),[28], Ni(II)[25], Cu(II),[21] Ga(III)[29]). The basic coordination motif consists of 3 cations connected together by 3 gallates ligands, all lying roughly in the same plane to define a triangle (see Figure 1). Depending on their nature, oxidation state and surrounding solvent molecules, the cations could adopt either an octahedral or a square pyramidal coordination. As observed in other pyrogallate coordination compounds,[13,15,16] remaining protons on the meta-oxygen atoms commonly maintain the charge balance.[21,26–30] Based on the similarities of their crystal structures, it was also initially proposed that the formation of such a coordinative assembly arose from the insertion of cations within a preformed metal-free hydrogen-bonded capsule;[21] nevertheless, deeper analyses found that such assemblies could also rearrange in solution.[25,31] To the best of our knowledge, these trismetallic units have never been observed in other compounds than these capsules. We recently showed that when associated with Zr(IV), pyrogallate derivatives afford a chain-like coordination motif built up from ZrO_8 polyhedra for a very broad range of ligands and experimental conditions.[14–16] In a similar way, we wonder if the afore mentioned triangular units, found with 5 to 6-fold coordinated cations, are specific to

[a] Institut des Matériaux Jean Rouxel (IMN), Université de Nantes, CNRS UMR 6502, 2 rue de la Houssinière, BP 32229, 44322 Nantes cedex 3, France. Email : thomas.devic@cnrs-imn.fr.
[a] Instituto de Ciencia Molecular (ICMol), c/Catedrático José Beltrán, 2, 46980 Paterna, Spain.
[b] Facultad de Ingeniería, Ciencia y tecnología, Depto. Matemáticas y Ciencias de la Ingeniería, Universidad Bernardo O'Higgins, Chile.

† Electronic Supplementary Information (ESI) available: syntheses, structure determination, detailed characterizations. See DOI: 10.1039/x0xx00000x

the set of macrocyclic ligands mentioned earlier, or could also be formed with other gallate derivatives, and ultimately be used as a secondary building unit to build up extended coordination networks.[32]

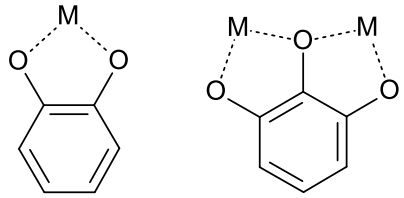

Scheme 1. Typical catecholate (left) and gallate (right) coordination motif.

From a materials viewpoint, considering the non-innocent character of phenolate ligands,[33] such building units could ultimately afford interesting electronic or magnetic properties. We here first systematically investigated the reactivity of vanadium salts with the simplest pyrogallate derivate, namely pyrogallol. We show that the $V_3(pgal)_3^{3-}$ triangular unit is easily formed in a broad set of experimental conditions. The structures of two of these complexes will be presented, together with their redox activities, both in solution and in the solid state. Ultimately, their magnetic behaviour, both in static and dynamic conditions, will be discussed.

Results and discussion

Synthesis, structure and spectroscopic characterization

A survey of the Cambridge Structural Database indicated the existence of a single crystalline compound combining vanadium and pgal, namely a bimetallic complex combining both acetylacetonate (acac) and H_3pgal ligand which was prepared in tetrahydrofuran.[34] Thanks to a solvothermal high-throughput setup,[35] the reactivity of pyrogallol (H_3pgal) with vanadium salts was here systematically screened in three polar solvents (water, methanol and N,N-dimethylformamide (DMF)) starting from either V(+III) (VCl_3), V(+IV) ($VO(SO_4).H_2O$, $VO(acac)_2$) or V(V) (V_2O_5, $(NH_4)VO_3$) at various pH. Only vanadyl acetylacetonate[36] afforded crystalline solids, both in methanol and DMF. The further optimization of other experimental parameters, such as temperature (60 and 120°C for methanol and DMF respectively) and ligand-to-metal-to-base (here aqueous KOH) ratio (1:1:2) ultimately yielded samples suitable for single crystal X-ray diffraction (XRD) analyses. Details about the structure determination can be found in Supporting Information (Table S1).

Both compounds, formulated $K_3V_3O_3(pgal)_3{\cdot}2(DMF)$ and $K_3V_3O_3(pgal)_3{\cdot}4(H_2O)$, consist of the same tris-anionic tris-metallic complex built up from three fully deprotonated pyrogallates, and three vanadyl motifs (Figure 1a). While the synthesis carried out in DMF lead to a pure DMF solvate, in the case of methanol, structure determination unambiguously indicates the presence of water molecules only, likely coming from the aqueous KOH solution. Each vanadium is bound to two pyrogallate ligands as well as one terminal oxygen atom, and adopts a square pyramidal coordination. Analyses of the bond distances, as well as bond distances calculations[37] (see Table S2) indicate a +IV oxidation state for each vanadium ion, in line with the coordination geometry and the presence of terminal vanadyl bonds (V=O distances are in the range 1.598(4)-1.623(4) Å). Each ligand binds to two V(IV) cations through the standard coordination motif depicted Scheme 1. This ultimately defines a bowl-shaped complex presenting a pseudo 3-fold axis, with the three vanadyl bonds pointing outside of the cavity (Figure 1b).

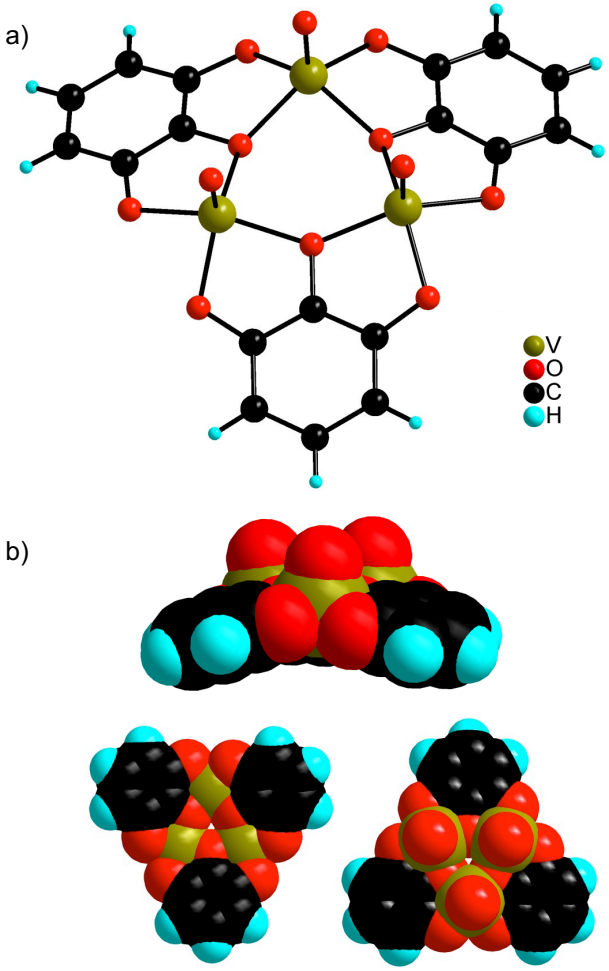

Figure 1. Structure of the $V_3O_3(pgal)_3^{3-}$ complex. a) ball and stick representation; b) van der Waals representations, highlighting its bowl-like shape.

This motif is almost identical to the one observed by Yuan *et al.* in the capsule $(VO)_{24}(PgC_n)_6$ (ball forms).[27] Notably, this ball shape is very similar, with a distance between the plane defined by the 3 aromatic rings and the vanadium atoms lying in the 0.9-1.1 Å range in both cases (see Figure S3). While in the capsules, the charge balance relies on remaining phenolic protons,[21,26–30] the structures of both solvates here contain 3 potassium cations per complex. Their presence was indeed confirmed by scanning electron microscopy - energy-dispersive X-ray spectroscopy (SEM-EDXS) analysis, which gives a V to K ratio equal to 1 (Figure S5), in accordance with the structure refinement. These cations are weakly interacting with oxygen atoms arising from pyrogallates, vanadyls and solvent molecules (see Table S3 for

K-O distances and Figure S1). For the DMF solvate, one of the potassium ion (K3) is also involved in a cation-π interaction with the pyrogallate ring,[38,39] as already found in gallate[17] and pyrogallate[40] derivatives. A similar feature might occur for potassium ion K2 in the hydrate, although in an "off-axis" configuration[41] (see Table S4 and Figure S2).

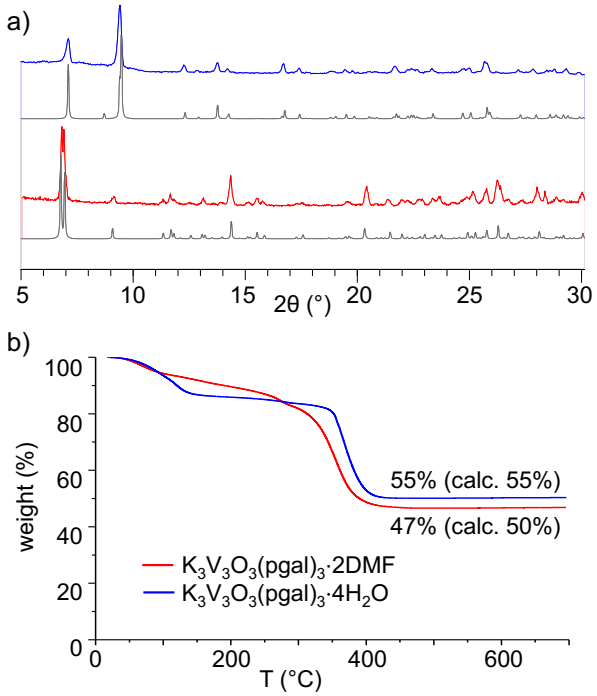

Figure 2. Structural and chemical characterizations of $K_3V_3O_3(pgal)_3·2(DMF)$ (red) and $K_3V_3O_3(pgal)_3·4(H_2O)$ (blue). a) X-ray powder patterns, compared with the ones calculated from the single crystal data (black); b) thermogravimetric analyses performed under O_2.

The comparison of the experimental X-ray powder diffraction (XRPD) with the one calculated from the single crystal data indicated that both solids are obtained in a pure form (see Figure 2a). Both compounds were also analyzed by thermogravimetric analyses carried out under oxygen (Figure 2b). After a first weight loss at low temperature (<200°C) associated with solvent departure, the full combustion occurred at 300-350°C to eventually afford V_2O_5 + K_2O. The experimental weight losses match well with the ones calculated from the proposed formula (see Figure 2b), confirming the purity of both the hydrate and DMF solvates. Both compounds were further characterized spectroscopically. Infrared spectroscopy first confirmed that free pyrogallol is absent in the final products (Figure 3a). Furthermore, the presence of strong bands at ca. 970-930 cm^{-1} is indicative of the presence of V=O bonds (V=O vibration band expected in the range 930-1030 cm^{-1}),[36,42,43] although an overlap with a band belonging to the ligand cannot be totally ruled out. Raman spectra were also collected, both in the ranges 1720-620 and 1260-60 cm^{-1}, with the final aim at identifying bands specific to the triangular $V_3O_3(pgal)_3$ motif. Contrary to pyrogallol alone, both complexes were found to be very beam-sensitive upon irradiation at 514 and 633 nm; only an irradiation at 785 nm afforded reasonably stable signals (Figures 3b and S4). At low wavenumber, bands at 382, 285 and 256 cm^{-1} which are not visible for the free ligand, were found in both compounds; the first one can be tentatively be assigned to the V-O vibration while the other ones might be associated with deformation modes.[44] At higher wavenumbers (Figure S4) a strong peak centered at 970 cm^{-1} was observed in both solvates, and was attributed to the V=O vibration.

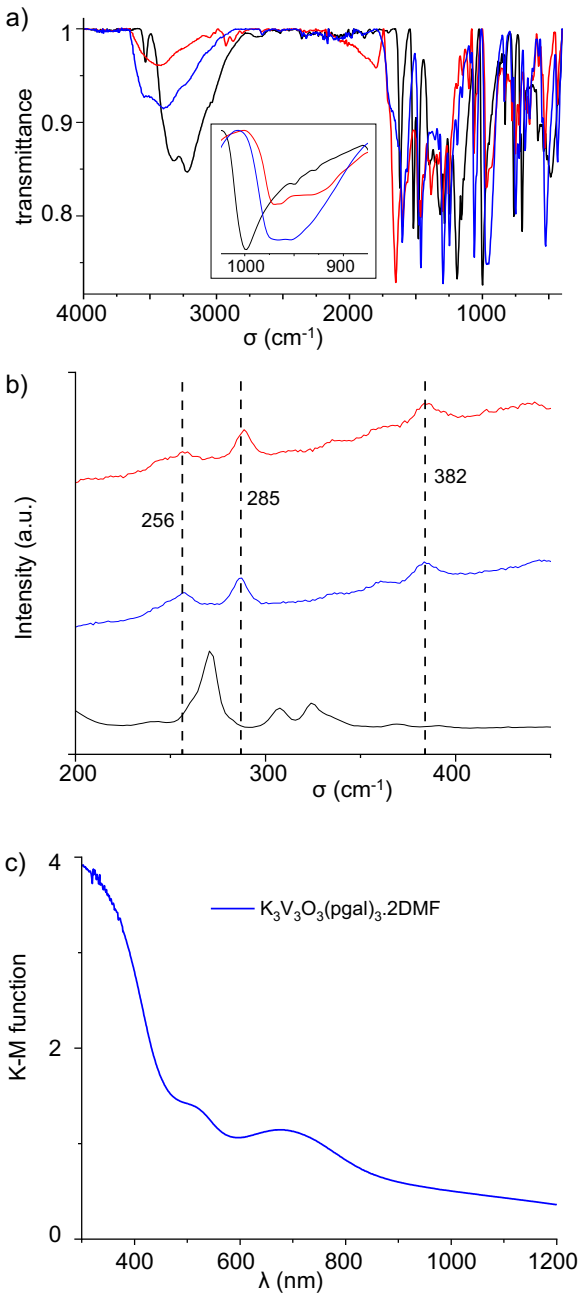

Figure 3. Spectroscopic characterizations of $K_3V_3O_3(pgal)_3·2(DMF)$ (blue) and $K_3V_3O_3(pgal)_3·4(H_2O)$ (red) as compared to the free ligand H_3pgal (black). a) Infrared spectra (inset: zoom in the 1000-900 cm^{-1} region); b) Raman spectra upon irradiation at 785 nm; c) UV-vis solid state reflectance spectrum of $K_3V_3O_3(pgal)_3·2(DMF)$.

Solid state UV-vis reflectance spectroscopy evidenced the presence of two absorption bands centered at *ca.* 510 and 684 nm (broad), in the expected range for oxovanadium-phenolate complexes.[45]

To summarize, all spectroscopic characterizations are in good agreement with the structure extracted from the single crystal analysis, and the assignment of the oxidation state of the cation and the ligand.

Electrochemical properties

As both the organic gallate derivative[46] and the vanadium cation *a priori* hold a redox activity, the electrochemical properties of the title solids were investigated, initially in the solid state. Although numerous studies have already evidenced the rich electrochemistry of vanadium phenolates complexes in solution in line with the non-innocent character of this family of ligands,[42,47–53] to the best of our knowledge no report in the solid state is available to date. Standard two electrodes Swagelok cells commonly used to evaluate active materials for Li-ion batteries were used, together with a lithium metal counter electrode and 1M $LiPF_6$ in a 1:1 mixture of ethylenecarbonate and propylenecarbonate electrolyte (see Supporting Information for details). The complex (here the hydrate) was first dried at 120 °C under vacuum to get rid of the solvent molecules. Considering the redox species at play, the solid was evaluated both in oxidation (between 2.5 and 4 V *vs.* Li^+/Li) and in reduction (between 1.0 and 3.0 V *vs.* Li^+/Li). Data are shown Figure 4a. Upon oxidation (plain line), a continuous event spanning from 3.4 to 4.0 V is observed, with an inflection point at ~ 3.7 V. This oxidation corresponds to the exchange of 4 electrons per trimeric unit (1.3 electrons per V) and could thus be tentatively attributed to the oxidation of both V(IV) cations and pyrogallate moieties.

Considering the redox potential of Li^+/Li (-3.04 V vs NHE), this oxidation potential rather matches with those measured in solution for square pyramidal oxovanadium-phenolate complexes.[53,54] Nevertheless, this oxidation is found to be irreversible upon further reduction and cycling. Scanning a narrower potential range (2.8-3.7 V vs. Li^+/Li) to possibly address a single redox event leads to a reduced number of electron exchanged (~1.5 per trimeric unit) but without any improvement of the reversibility (Figure S6). On the reduction side (Figure 4a, dashed line), a single event at ~ 1.5 V vs. Li^+/Li is detected, and associated with 1 electron exchanged per trimeric unit. Although occurring at a rather low potential, this reduction might be related to the V(IV)/V(III) redox couple.[53] Similarly to the oxidation, the reduction was found to be irreversible, precluding the use of this compound as active electrode materials in ions-batteries. A postmortem inspection of the electrodes evidenced the solubilization of the material, which could at a first sight be attributed to its molecular (rather than polymeric) character, and explains such an irreversibility. To determine whether this solubilization is the sole source of irreversibility, further experiments were carried out in aqueous solution (electrolyte: 1 M $MClO_4$, M = Li, Na), where both complexes are soluble. Both solvates were studied by cyclic voltammetry between -0.6 and 1.2 V *vs*. AgCl/Ag (see Figure S7). As they present similar electrochemical traces, only the hydrate will be discussed (Figure 4b). Experiments were first carried out at the natural pH (~4-5). No event is detected in reduction, while two oxidation waves are observed at *ca.* 0.5 and 0.98 V vs. AgCl/Ag. Considering the redox potential of AgCl/Ag (0.205 V vs NHE), these potentials are rather in line with those observed in the solid state, and hence attributed to the oxidation of both the ligand and the cation. Upon addition of an excess of base (here trimethylamine), the first oxidation I is strongly downshifted to 0.02 V (ΔE = 0.48 V), while the one at high potential (II) is less affected (ΔE = 0.10 V), suggesting that proton transfer is involved at least in the first process. In all cases, both processes were found to be irreversible (see also Figure S8), suggesting that the title complex is intrinsically unstable upon oxidation.

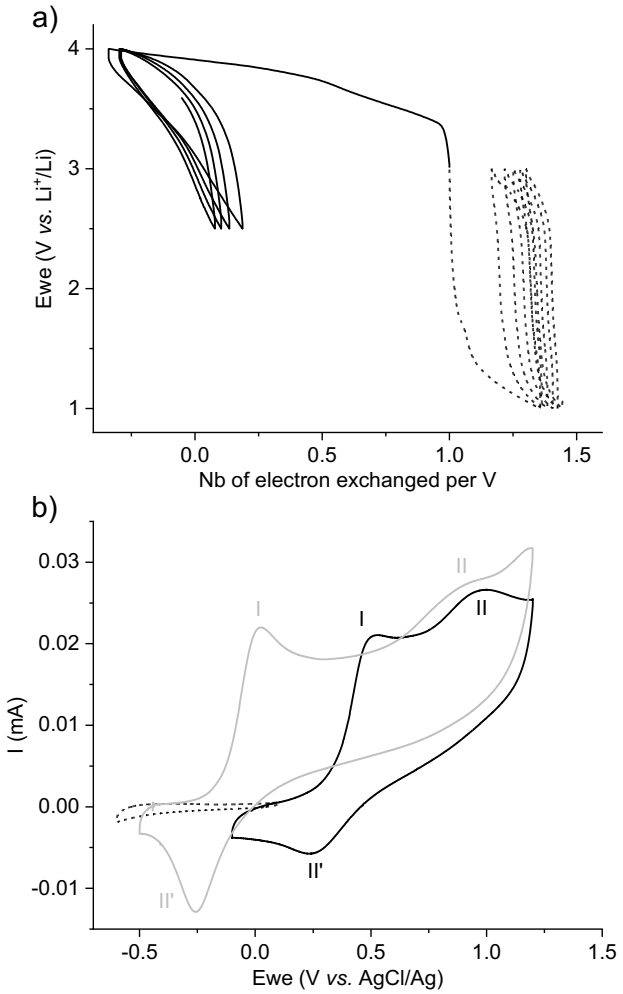

Figure 4. Electrochemical properties of $K_3VO_3(pgal)_3{\cdot}4H_2O$. a) In the solid state (dried complex): redox potential vs number of electron exchanged under galvanostatic conditions both upon oxidation (plain line) and reduction (dashed line); b) in aqueous solution (hydrated complex, electrolyte 1 M $NaClO_4$); black: dissolved in water (pH~4-5), upon oxidation (plain line) and reduction (dashed line); grey: after the addition of 10 equivalents of trimethylamine (pH~11).

Magnetic properties

Eventually, the magnetic properties of the title complex were investigated. Static magnetic measurements (dc) were first performed upon immersing crystals of a fresh sample of $K_3V_3O_3(pgal)_3{\cdot}4(H_2O)$ in MeOH from 2 to 300 K under a magnetic field of 1000 G. Data are shown Figure 5a. The room temperature $\chi_m T$ value of 1.09 $cm^3{\cdot}K{\cdot}mol^{-1}$ (where χ_m is the

molar magnetic susceptibility) is close to the expected value of 1.08 $cm^3 \cdot K \cdot mol^{-1}$ for 3 non-interacting V(IV) centers with a g = 1.97,[55] hence in full agreement with the structural and spectroscopic analyses. This value is continuously increasing upon decreasing temperature reaching a maximum of 1.50 $cm^3 \cdot K \cdot mol^{-1}$ at 7 K and subsequently decreases sharply to 1.11 $cm^3 \cdot K \cdot mol^{-1}$ at 2.0 K. The increase of the $\chi_m T$ value upon reduction of the temperature indicates the existence of ferromagnetic interactions between the V(IV) centers. The dc magnetic data was fitted to the following analytical experimental equation[56] using the PHI program.[57]

$$\hat{H} = -2J(S_1S_2 + S_1S_3 + S_2S_3) + \mu_B gH \sum_{i=1}^{3} \hat{S}_i - zJ`\langle S_4 \rangle \sum_{i=1}^{3} \hat{S}_i$$

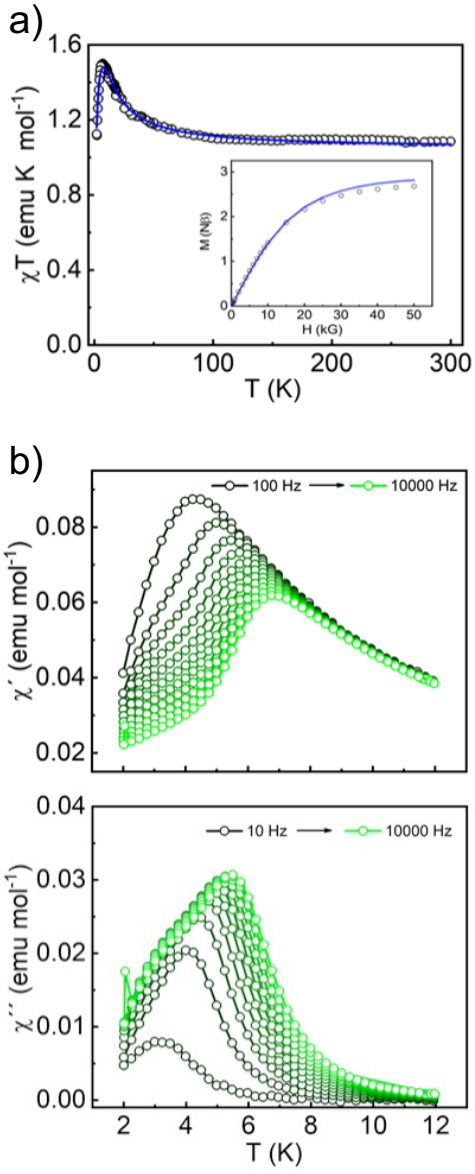

Figure 5. Magnetic behavior of of $K_3VO_3(pgal)_3$. a) Thermal dependence of $\chi_m T$ at 1000 G between 2 to 300 K, with the curve for the best fit parameters obtained considering equation above. Inset, M(H) plot at 2 K with the calculated magnetization curve using the same Hamiltonian; b) *ac* susceptibility (χ´(T) and χ´´(T)) measurement at different frequencies and at a *dc* magnetic field of 6000 G.

The model considers the isotropic interactions *J* for an equilateral triangle and the secondary intermolecular interaction *zJ´*. The best fit parameters show a ferromagnetic exchange interaction *J* = +4.92 (9) cm^{-1} occurring between the V(IV) centers and an antiferromagnetic intermolecular interaction among molecules of -0.15 cm^{-1} (g = 1.97). The ferromagnetic nature of the *J* value is in agreement with the observed in a V_{24} capsule containing the same trimeric unit.[27] In our system, this exchange interaction may be also influenced to some extent by the presence of the K^+ ions that interact with the oxygen of the vanadyl unit, which are known to determine the overlap between the magnetic ions (V(IV)), by tuning the interaction between them.[59]

Dynamic magnetic measurements (ac) in the absence of an external dc field show the absence of an out-of-phase signal, χ'' (Figure S9), as reported previously.[27] However, upon the application of different dc fields (500-6000 G), frequency-dependent signals in the out-of-phase are present. This is possibly due to the presence of a fast relaxation of the magnetisation through a quantum tunnelling mechanism that can be easily removed with the application of an external dc field that drives the levels away from the hyperfine avoided crossing region causing the magnetic uniaxial anisotropy in this system.[60] Analysis of the field dependence of the compound suggest that a high dc field (6000 G) is necessary to properly study the relaxation dynamics (Figure S9). Thus, in ac measurements performed in the presence of an external dc field of 6000 G, both χ' and χ'' show slow relaxation and a maximum which is frequency dependent, as depicted in the χ´´(T) and χ´´(υ) curves (Figure 5b). Analysis of the frequency dependence of the χ'' peaks through an Arrhenius plot permits estimation of the magnetisation-relaxation parameters in this system (Figure S10). However, afforded the large external field applied, these values become physically meaningless.

Conclusions

We here described the synthesis of a new trismetallic vanadium complex, its structural and spectroscopic characterization, as well as its redox and magnetic properties. The formation of polymetallic vanadium complexes is usually very condition dependent.[64] Here, we found that the combination of the gallate unit and V(IV) leads easily to the formation of the title complex, not only with pyrogallol[4]arene as already reported,[27] but also with the simplest pyrogallate derivative. This trimetallic complex even appears rather robust, as it is formed in different experimental conditions (solvent, temperature), and furthermore accept various charges (anionic and neutral[27]). It seems thus reasonable to postulate that such a trimetallic unit might also be present in amorphous coordination coatings made from gallate derivatives, especially when vanadium is used;[65] our spectroscopic data might help to identify this motif in such complex mixtures. We have studied the magnetic properties of the $V_3O_3(pgal)_3$ unit, which exhibits intramolecular ferromagnetic interactions. Eventually, the $V_3O_3(pgal)_3$ unit also appears as a new potential molecular inorganic secondary building unit (ISBU) for the construction of extended magnetic coordination networks. Whereas many ISBU

based on carboxylate ligands have been identified and used for the construction of extended networks,[32] phenolate ligands and polymetallic entities are extremely rare, although they offer clear benefits in term of chemical stability, effective magnetic interactions or redox properties.[7–9,15] Such investigations are currently under way in our laboratory.

Conflicts of interest

There are no conflicts to declare.

Acknowledgements

Funding from the region Pays de la Loire (project PSR 'MatHySE2') is acknowledged. The authors also thank the synchrotron Soleil for providing access to the beamline Cristal Soleil, as well as the network Reciprocs. P. Fertey is thanked for this help during the measurement and G. Mouchaham for fruitful discussions.

Notes and references

1 M. A. Rahim, S. L. Kristufek, S. Pan, J. J. Richardson and F. Caruso, *Angew. Chem. Int. Ed.*, 2019, **58**, 1904–1927.
2 M. Shin, E. Park and H. Lee, *Adv. Funct. Mater.*, 2019, **29**, 1903022.
3 M. Björnmalm, L. M. Wong, J. P. Wojciechowski, J. Penders, C. C. Horgan, M. A. Booth, N. G. Martin, S. Sattler and M. M. Stevens, *Chem. Sci.*, 2019, **10**, 10179–10194.
4 C. G. Pierpont, *Inorg. Chem.*, 2011, **50**, 9766–9772.
5 S. Quideau, D. Deffieux, C. Douat-Casassus and L. Pouységu, *Angew. Chem. Int. Ed.*, 2011, **50**, 586–621.
6 T. J. Boyle, L. J. Tribby, T. M. Alam, S. D. Bunge and G. P. Holland, *Polyhedron*, 2005, **24**, 1143–1152.
7 S. Leubner, V. E. G. Bengtsson, A. K. Inge, M. Wahiduzzaman, F. Steinke, A. Jaworski, H. Xu, S. Halis, P. Rönfeldt, H. Reinsch, G. Maurin, X. Zou and N. Stock, *Dalton Trans.*, 2020, **49**, 3088–3092.
8 R. Matheu, E. Gutierrez-Puebla, M. Á. Monge, C. S. Diercks, J. Kang, M. S. Prévot, X. Pei, N. Hanikel, B. Zhang, P. Yang and O. M. Yaghi, *J. Am. Chem. Soc.*, 2019, **141**, 17081–17085.
9 M. P. M. Poschmann, H. Reinsch and N. Stock, *Z. Anorg. Allg. Chem.*, 2021, **647**, 436–441.
10 B. Aurivillius and C. Särnstrand, *Acta Chem. Scand. A*, 1976, **30**, 232–234.
11 C.-H. Wunderlich, R. Weber and G. Bergerhoff, *Z. Anorg. Allg. Chem.*, 1991, **598**, 371–376.
12 R. K. Feller and A. K. Cheetham, *Solid State Sci.*, 2006, **8**, 1121–1125.
13 P. J. Saines, H. H. M. Yeung, J. R. Hester, A. R. Lennie and A. K. Cheetham, *Dalton Trans.*, 2011, **40**, 6401–6410.
14 L. Cooper, N. Guillou, C. Martineau, E. Elkaim, F. Taulelle, C. Serre and T. Devic, *Eur. J. Inorg. Chem.*, 2014, 6281–6289.
15 G. Mouchaham, L. Cooper, N. Guillou, C. Martineau, E. Elkaïm, S. Bourrelly, P. L. Llewellyn, C. Allain, G. Clavier, C. Serre and T. Devic, *Angew. Chem. Int. Ed.*, 2015, **54**, 13297–13301.
16 G. Mouchaham, B. Abeykoon, M. Giménez-Marqués, S. Navalon, A. Santiago-Portillo, M. Affram, N. Guillou, C. Martineau, H. Garcia, A. Fateeva and T. Devic, *Chem. Commun.*, 2017, **53**, 7661–7664.
17 T. Hidalgo, L. Cooper, M. Gorman, T. Lozano-Fernández, R. Simón-Vázquez, G. Mouchaham, J. Marrot, N. Guillou, C. Serre, P. Fertey, Á. González-Fernández, T. Devic and P. Horcajada, *J. Mater. Chem. B*, 2017, **5**, 2813–2822.
18 E.-X. Chen, M. Qiu, Y.-F. Zhang, Y.-S. Zhu, L.-Y. Liu, Y.-Y. Sun, X. Bu, J. Zhang and Q. Lin, *Adv. Mater.*, 2018, **30**, n/a-n/a.
19 L. Cooper, T. Hidalgo, M. Gorman, T. Lozano-Fernandez, R. Simon-Vazquez, C. Olivier, N. Guillou, C. Serre, C. Martineau, F. Taulelle, D. Damasceno-Borges, G. Maurin, A. Gonzalez-Fernandez, P. Horcajada and T. Devic, *Chem. Commun.*, 2015, **51**, 5848–5851.
20 N. P. Power, S. J. Dalgarno and J. L. Atwood, *Angew. Chem. Int. Ed.*, 2007, **46**, 8601–8604.
21 R. M. McKinlay, G. W. V. Cave and J. L. Atwood, *Proc. Natl. Acad. Sci.*, 2005, **102**, 5944–5948.
22 K. Su, M. Wu, Y. Tan, W. Wang, D. Yuan and M. Hong, *Chem. Commun.*, 2017, **53**, 9598–9601.
23 A. S. Rathnayake, H. W. L. Fraser, E. K. Brechin, S. J. Dalgarno, J. E. Baumeister, J. White, P. Rungthanaphatsophon, J. R. Walensky, C. L. Barnes, S. J. Teat and J. L. Atwood, *Nat. Commun.*, 2018, **9**, 2119.
24 A. S. Rathnayake, H. W. L. Fraser, E. K. Brechin, S. J. Dalgarno, J. E. Baumeister, J. White, P. Rungthanaphatsophon, J. R. Walensky, S. P. Kelley, C. L. Barnes and J. L. Atwood, *J. Am. Chem. Soc.*, 2018, **140**, 15611–15615.
25 H. Kumari, A. V. Mossine, S. R. Kline, C. L. Dennis, D. A. Fowler, S. J. Teat, C. L. Barnes, C. A. Deakyne and J. L. Atwood, *Angew. Chem. Int. Ed.*, 2012, **51**, 1452–1454.
26 C. Zhang, R. S. Patil, T. Li, C. L. Barnes and J. L. Atwood, *Chem. Commun.*, 2017, **53**, 4312–4314.
27 K. Su, M. Wu, D. Yuan and M. Hong, *Nat. Commun.*, 2018, **9**, 4941.
28 A. S. Rathnayake, K. A. Feaster, J. White, C. L. Barnes, S. J. Teat and J. L. Atwood, *Cryst. Growth Des.*, 2016, **16**, 3562–3564.
29 R. M. McKinlay, P. K. Thallapally, G. W. V. Cave and J. L. Atwood, *Angew. Chem. Int. Ed.*, 2005, **44**, 5733–5736.
30 R. M. McKinlay, P. K. Thallapally and J. L. Atwood, *Chem. Commun.*, 2006, 2956–2958.
31 H. Kumari, C. A. Deakyne and J. L. Atwood, *Acc. Chem. Res.*, 2014, **47**, 3080–3088.
32 D. J. Tranchemontagne, J. L. Mendoza-Cortes, M. O'Keeffe and O. M. Yaghi, *Chem. Soc. Rev.*, 2009, **38**, 1257–1283.
33 W. Kaim, *Inorg. Chem.*, 2011, **50**, 9752–9765.
34 S. Lee, K. Nakanishi, M. Y. Chiang, R. B. Frankel and K. Spartalian, *J. Chem. Soc., Chem. Commun.*, 1988, **0**, 785–786.
35 N. Stock, *Micro. Meso. Mater.*, 2010, **129**, 287–295.
36 M. R. Maurya, *Coord. Chem. Rev.*, 2003, **237**, 163–181.
37 N. E. Brese and M. O'Keeffe, *Acta Cryst. B*, 1991, **47**, 192–197.
38 D. A. Dougherty, *Acc. Chem. Res.*, 2013, **46**, 885–893.
39 A. S. Mahadevi and G. N. Sastry, *Chem. Rev.*, 2013, **113**, 2100–2138.
40 A. Åhman and M. Nissinen, *Chem. Commun.*, 2006, 1209–1211.
41 M. S. Marshall, R. P. Steele, K. S. Thanthiriwatte and C. D. Sherrill, *J. Phys. Chem. A*, 2009, **113**, 13628–13632.
42 S. R. Cooper, Y. B. Koh and K. N. Raymond, *J. Am. Chem. Soc.*, 1982, **104**, 5092–5102.
43 M. Atzori, S. Benci, E. Morra, L. Tesi, M. Chiesa, R. Torre, L. Sorace and R. Sessoli, *Inorg. Chem.*, 2018, **57**, 731–740.
44 A. H. Jubert, R. P. Diez, S. B. Etcheverry and E. J. Baran, *J. Raman Spectro.*, 1993, **24**, 627–631.
45 M. J. Sever and J. J. Wilker, *Dalton Trans.*, 2004, 1061–1072.

46 C.-H. Hung, W.-T. Chang, W.-Y. Su and S.-H. Cheng, *Electroanal.*, 2014, **26**, 2237–2243.
47 C. Drouza and A. D. Keramidas, *Inorg. Chem.*, 2008, **47**, 7211–7224.
48 B. Baruah, S. Das and A. Chakravorty, *Inorg. Chem.*, 2002, **41**, 4502–4508.
49 G. Asgedom, A. Sreedhara, C. P. Rao and E. Kolehmainen, *Polyhedron*, 1996, **15**, 3731–3739.
50 M. Shit, S. Maity, S. Bera, T. Weyhermüller and P. Ghosh, *New J. Chem.*, 2016, **40**, 10305–10315.
51 S. Kundu, S. Maity, A. N. Maity, S.-C. Ke and P. Ghosh, *Dalton Trans.*, 2013, **42**, 4586–4601.
52 S. Kundu, S. Maity, T. Weyhermüller and P. Ghosh, *Inorg. Chem.*, 2013, **52**, 7417–7430.
53 P. Galloni, V. Conte and B. Floris, *Coord. Chem. Rev.*, 2015, **301–302**, 240–299.
54 M. Vlasiou, C. Drouza, T. A. Kabanos and A. D. Keramidas, *J. Inorg. Biochem.*, 2015, **147**, 39–43.
55 K. Muñoz-Becerra, P. Hermosilla-Ibáñez, E. Le Fur, O. Cador, V. Paredes-García, E. Spodine and D. Venegas-Yazigi, *Cryst. Growth Des.*, 2015, **15**, 2561–2564.
56 Kahn, Olivier, *Molecular Magnetism*, VCH, Weinheim, Germany, 1993.
57 N. F. Chilton, R. P. Anderson, L. D. Turner, A. Soncini and K. S. Murray, *J. Comput. Chem.*, 2013, **34**, 1164–1175.
58 A. Rodríguez-Fortea, P. Alemany, S. Alvarez and E. Ruiz, *Eur. J. Inorg. Chem.*, 2004, **2004**, 143–153.
59 P. Hermosilla-Ibáñez, W. Cañon-Mancisidor, J. Costamagna, A. Vega, V. Paredes-García, M. T. Garland, E. L. Fur, O. Cador, E. Spodine and D. Venegas-Yazigi, *Dalton Trans.*, 2014, **43**, 14132–14141.
60 N. Ishikawa, M. Sugita and W. Wernsdorfer, *J. Am. Chem. Soc.*, 2005, **127**, 3650–3651.
62 H. Kumari, C. L. Dennis, A. V. Mossine, C. A. Deakyne and J. L. Atwood, *ACS Nano*, 2012, **6**, 272–275.
63 H. Kumari, C. L. Dennis, A. V. Mossine, C. A. Deakyne and J. L. Atwood, *J. Am. Chem. Soc.*, 2013, **135**, 7110–7113.
64 M. R. Maurya, *Coord. Chem. Rev.*, 2019, **383**, 43–81.
65 J. Guo, Y. Ping, H. Ejima, K. Alt, M. Meissner, J. J. Richardson, Y. Yan, K. Peter, D. von Elverfeldt, C. E. Hagemeyer and F. Caruso, *Angew. Chem. Int. Ed.*, 2014, **53**, 5546–5551.